



MODELING OF POST-BUCKLING BEHAVIOR OF CIRCULAR HOLLOW STEEL STUB COLUMNS

Hua Zhao⁽¹⁾, Chang Yang⁽²⁾, Zhixiang Yu⁽³⁾, Shichun Zhao⁽⁴⁾, Yuping Sun⁽⁵⁾

⁽¹⁾ Chengdu in China , Technology University of Chengdu & Southwest Jiaotong University , 584364542@qq.com

⁽²⁾ Chengdu in China , Southwest Jiaotong University , yangchang327@126.com

⁽³⁾ Chengdu in China , Southwest Jiaotong University , yzxzrq@home.swjtu.edu.cn

⁽⁴⁾ Chengdu in China , Southwest Jiaotong University , zhaosc1961@163.com

⁽⁵⁾ Kobe in Japan , Kobe University , sun@person.kobe-u.ac.jp

Abstract

A stress-strain model is proposed to define the relationship between axial compressive stress and strain for circular hollow steel stub (CHSS) columns, which have been widely used as predominant gravity-sustaining structural component in transportation terminal buildings. The proposed model consists of two curves, one of which is intended to depict the ascending branch and account for the effect of residual stress induced during the manufacturing process, and the other is to depict the descending portion and account for the effect of local buckling, either elastic or inelastic. Test results of thirty-five circular steel stub columns under monotonic axial compression are collected to calibrate and validate the model. The experiments were conducted in Japan and Australia. The previous tests of circular stub columns under concentric compression cover a wide range of structural factors such as D/t ratio and yield strength of steel tube. The D/t ratio ranged from 16.7 to 221, while the yield strength varied from 186 MPa to 835 MPa. Comparisons between the experimental stress-strain curves and theoretical results indicated that the proposed model could simulate compressive stress-strain behavior of CHSS columns up to large strain with very high accuracy.

Keywords: Circular hollow steel stub column, post buckling, stress-strain model



1. Introduction

Circular steel tube column (CSTC) has been well used as primary gravity-sustaining structural component in transportation terminal buildings located in earthquake-prone zones. In order to make full use of high strength and sound ductility of the steel, most of current design codes for steel structures put an upper limit upon the diameter-to-thickness (D/t) ratio of circular steel tubes. This upper limit is intended to ensure that local buckling of the steel tube does not occur before a CSTC under seismic loading develops its plastic moment-resisting capacity, which is generally referred to as plastic flexural strength (PFS).

However, lessons learnt from recent mega-earthquakes such as 2008 Sichuan earthquake and 2011 East Japan earthquake present a new challenge to modern steel structures. Building structures may be vibrated by much stronger ground motion than anticipated in current seismic codes. Under the ground motion stronger than anticipation, steel structures and components may experience larger deformation than the limit anticipated in current codes, resulting in unexpected local buckling in compressive CSTCs.

In addition, recently a potential mega-earthquake publicly named as Nankai-trough earthquake has gained more and more attention from the structural engineering community in Japan. The Nankai-trough earthquake is predicted to have a magnitude of at least 8.0^[1] and may cause strong ground motion with long-term natural period, leading to intense resonant vibration of the high-rise steel buildings. Hence, it is of urgent importance to understand seismic performance of steel structures under mega-earthquakes beyond anticipation. To analyze ultimate behavior of steel structures, a complete stress-strain model which can account for effect of local buckling on the compressive behavior of steel columns is indispensable. Unfortunately, none of the current design codes^[2-6] specify the post-local-buckling behavior of steel stub columns.

While there are several complete stress-strain models for square steel stub columns in the literatures^[7-9], no such a model for circular hollow steel stub (CHSS) columns exists at present. Many researchers have experimentally and analytically investigated the stress-strain behavior of CHSS columns under compression^[9-14], but most of the previous studies focused only on the local buckling strength and corresponding strain without analyzing the complete stress-strain curve.

The objective of this paper is to propose a complete stress-strain model for CHSS columns under compression. The proposed model consists of two curves. One curve is to predict the ascending portion and to trace the effect of the residual stress induced during manufacturing process of the CHSS, and the other is depict the post-local-buckling behavior.

2. Description of the previous experimental data

Experimental results of thirty-five CHSS columns^[12-15] under concentric compression are collected to calibrate and validate the proposed model. Fig. 1 shows the relationships between two structural factors and the measured peak stresses and the strains (ε_{sm}) at the peaks. Each measured peak stress shown in Fig. 1 represents the buckling strength of the stub column and is expressed in terms of strength ratio (S_{exp}), which is the ratio of the measured peak stress to the yield strength (f_{sy}) of steel. The test stub columns have identical aspect ratio of 3.0 in Japan and 3.5 in Australia, respectively.

As one can see from Fig. 1, the previous specimens cover a wide range of structural factors; the section diameter between 108 mm and 450 mm, the D/t ratio between 16.7 and 221, and the yield strength of steel between 186 MPa and 835 MPa, covering nearly all grades of CHSS available on the market.

3. Complete stress-strain model for CHSS columns under compression

As illustrated in Fig. 2, the proposed model consists of two curves. One curve is for the ascending branch and the other is for the descending portion. According to the proposed model, compressive stress (f_s) corresponding to a given compressive strain (ε_s) can be obtained as follows:

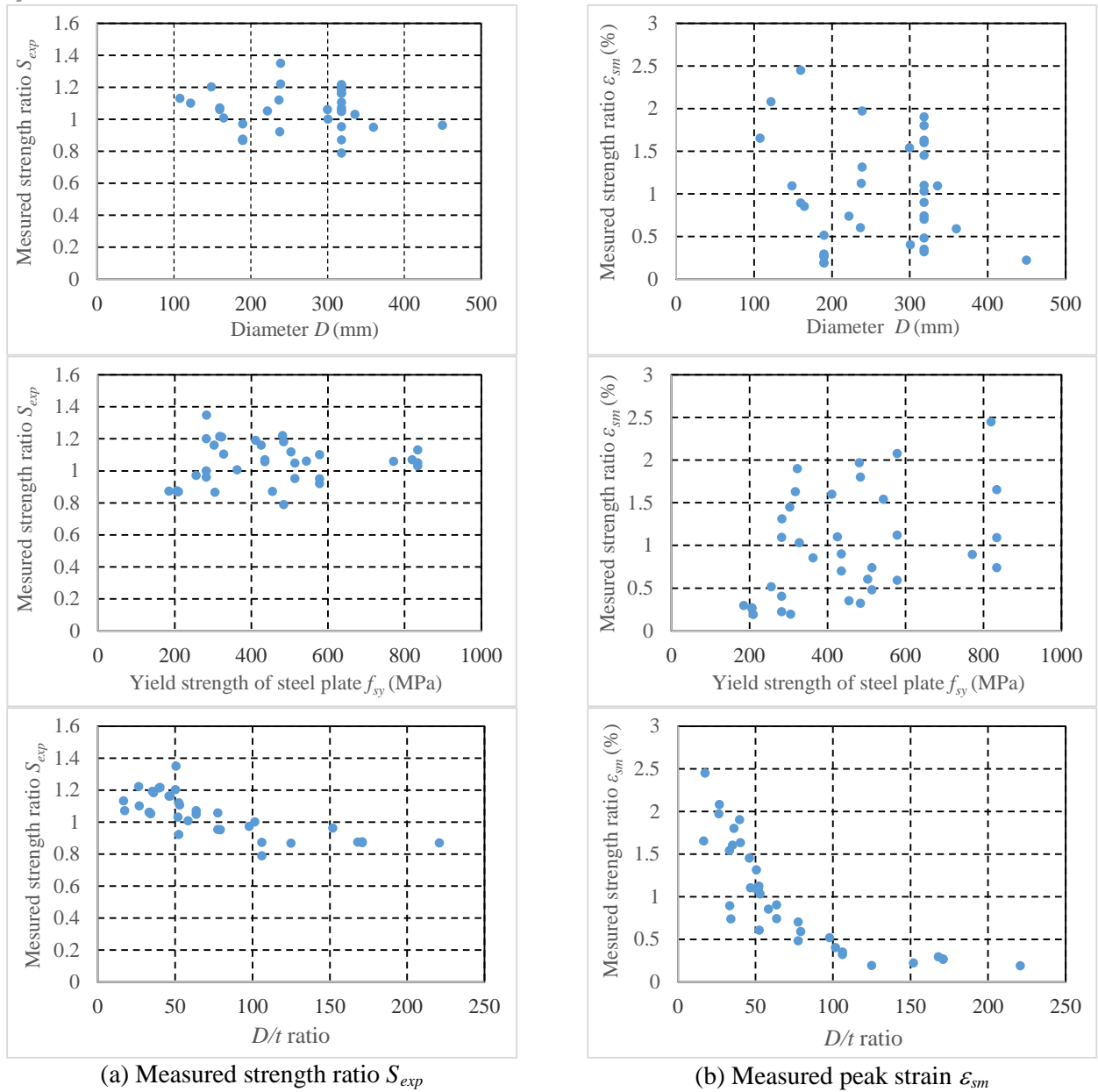


Fig. 1 – Distribution of the main experimental variables in previous tests

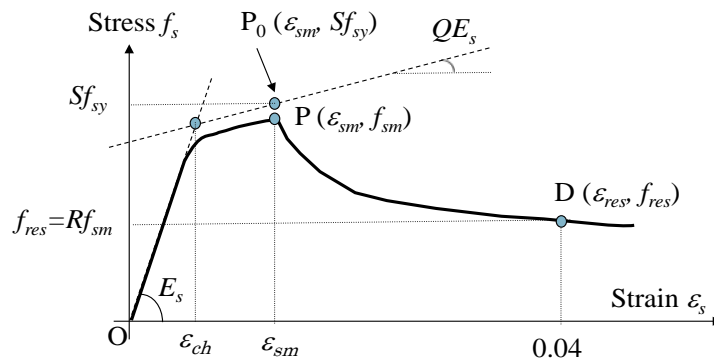


Fig. 2 – Outline of the proposed stress-strain model for CHSS columns under compression



$$f_s = \begin{cases} E_s \varepsilon_s \left(Q + \frac{1-Q}{\left(1 + |\varepsilon_s / \varepsilon_{ch}|^N\right)^{1/N}} \right), & \varepsilon_s \leq \varepsilon_{sm} \\ \frac{a}{b + \varepsilon_s}, & \varepsilon_s > \varepsilon_{sm} \end{cases} \quad (1)$$

Obviously, to completely determine the stress-strain relationship, three groups of parameters need to be fixed. They are, 1) parameters Q , N and ε_{ch} for the ascending portion, 2) stress f_{sm} and strain ε_{sm} to define the peak point P, and 3) a and b that govern the shape of the descending portion. Mathematical expressions of these parameters will be developed in the following sections.

3.1 The parameters defining the ascending portion

Eq. (1) is the well-known Menegotto-Pinto function that was originally proposed to predict Bauschinger's effect on the stress-strain behavior of steels under cyclically repeated loading^[16]. As the initial stiffness E_s (=205000 MPa) in Eq. (1) is known, only the second stiffness ratio Q (see Fig. 2) and the round coefficient N need to be fixed since the strain ε_{ch} , which is referred to as characteristic strain, can be calculated after fixing Q and N .

Based on the experimental investigation of monotonic and cyclic stress-strain behavior of dozens of reinforcing bars, one of the authors and his colleagues have developed equations to calculate Q and N for high-strength reinforcing bars that do not exhibit clear yield plateau. By modifying the equations proposed by Sun et al.^[17], the following equations are adopted to calculate Q and N for CHSS columns under compression.

$$Q = 0.1(\varepsilon_{sm})^{-2.5} \leq 0.005, \quad \varepsilon_{sm} \text{ in } \% \quad ; \quad N = 6.0 \quad (2)$$

After determining Q and N by Eq. (2), the characteristic strain ε_{ch} can be obtained as the abscissa of the intersection of the initial straight line and the straight line crosses the point P₀ (ε_{sm} , Sf_{sy}) with stiffness QE_s .

$$\varepsilon_{ch} = \frac{Sf_{sy} - QE_s \varepsilon_{sm}}{(1-Q)E_s} \quad (3)$$

Fig. 3 shows relationships between the measured strength ratio S_{exp} and two factors, the D/t ratio and the generalized diameter-to-thickness ratio α of steel tubes. The strength ratio S exhibits more pronounced correlation with α than D/t ratio. By conducting regression analysis of the test results shown in Fig. 3, the following equation is obtained to calculate the strength ratio S in Eq. (3).

$$S = \frac{1}{0.73 + 1.8\alpha}, \quad \alpha = \frac{D}{t} \frac{f_{sy}}{E_s} \quad (4)$$

3.2 The peak stress f_{sm} and peak strain ε_{sm}

To identify critical factors affecting peak strains ε_{sm} , Fig. 4 shows relationships between the measured ε_{sm} and D/t ratio as well as α of steel tubes. It should be noted that the measured ε_{sm} presented in the second graph in Fig.4 is normalized by yield strain ε_{sy} ($=f_{sy} / E_s$). The D/t ratio seems to exhibit stronger correlation with the experimental results than α . For the twenty-six specimens with D/t ratio less than 100, the coefficient of determination (R^2) between the measured ε_{sm} and D/t ratio, however, will decrease from 0.8571 to 0.6431. Based on this fact, Eq. (5) is derived to calculate the peak strain ε_{sm} .

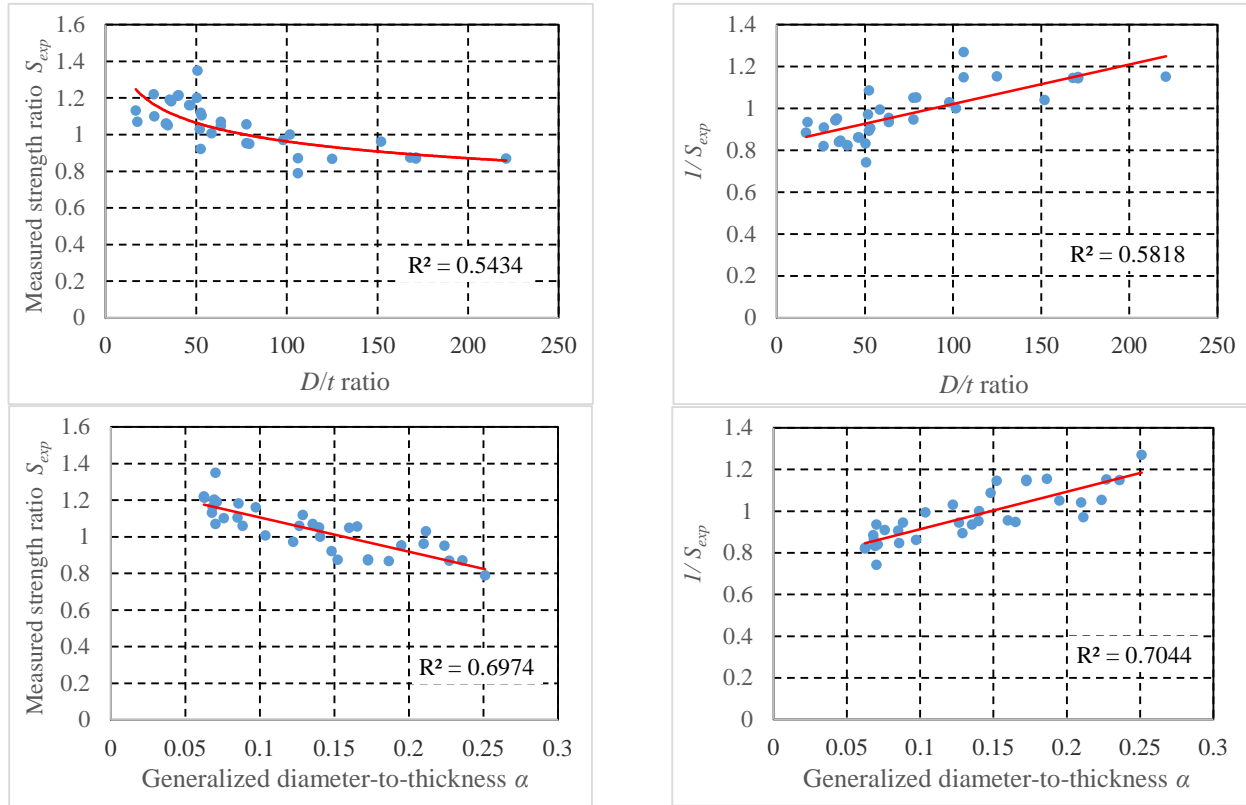


Fig. 3 – Relationships between the measured strength ratio S and main variables

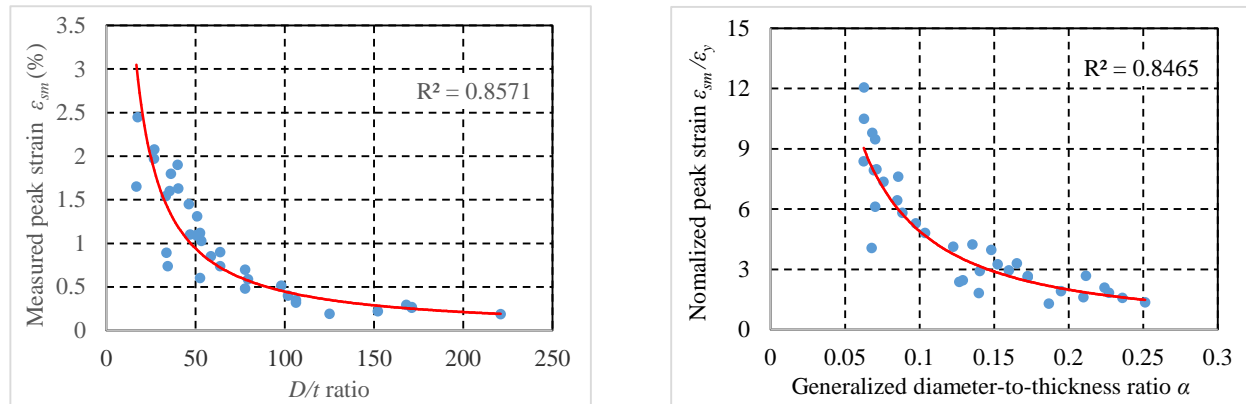


Fig. 4 – Relationships between the measured peak strain ϵ_{sm} and main variables

$$\frac{\epsilon_{sm}}{\epsilon_{sy}} = \frac{0.23}{\alpha^{1.3}} \quad (5)$$

After determining the peak strain ϵ_{sm} by Eq. (5), the peak stress f_{sm} can be obtained by substituting the determined ϵ_{sm} into Eq. (1) as follow:

$$f_{sm} = E_s \epsilon_{sm} \left(Q + \frac{1-Q}{\left(1 + |\epsilon_{sm}/\epsilon_{ch}|^N\right)^{1/N}} \right) \quad (6)$$

The peak stress f_{sm} obtained by Eq. (6) is the peak stress for the ascending portion, and will be also adopted as the peak stress for the descending portion in lieu of Sf_{sy} to ensure continuity of the two curves defined by Eq. (1) at the peak point P (see Fig. 2). Fig. 5 displays the influence of this replacement on the buckling strength of CHSS columns. The ordinate in Fig. 5 expresses the ratio of f_{sm} to Sf_{sy} .

Fig. 5 indicates that the ratio of f_{sm} to Sf_{sy} is over 0.99 for CHSS columns with α less than 0.25. The difference between f_{sm} in Eq. (8) and Sf_{sy} in Eq. (6) is about 1% on the conservative side. Such small difference is negligible from the viewpoint of practice, and implies validity of replacing Sf_{sy} with f_{sm} calculated by Eq. (8) as the peak stress of the descending portion.

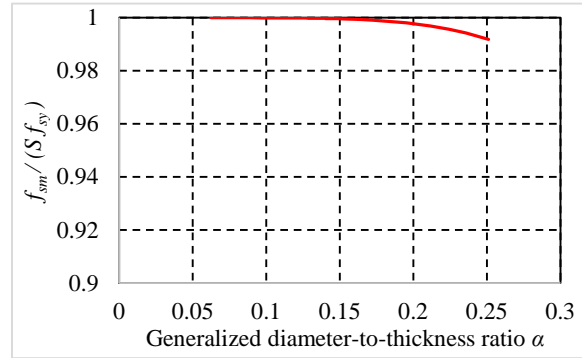


Fig. 5 – Comparison of the peak stress (f_{sm}) and the calculated buckling strength (Sf_{sy})

3.3 The parameters a and b for the descending portion

The two parameters governing the descending portion of the proposed model can be determined if the ordinates of two points on the descending curve are known. The descending curve must pass the peak point P (ϵ_{sm}, f_{sm}) (see Fig. 2) to maintain continuity with the ascending curve, and the other point at larger strain can be selected arbitrarily. It is rational to select a point where the decline in the compressive stress becomes sufficiently gentle. This point is expressed as point D (ϵ_{res}, f_{res}) in Fig. 2. Since previous experimental results have indicated that the local buckling is no longer critical in hollow steel stub columns if the peak strain was larger than 0.03^[18], this paper will take the strain of 0.04 as the abscissa ϵ_{res} of the point D. The remaining challenge is to determine the corresponding stress f_{res} , which is referred to as the residual strength hereafter.

Fig. 6 shows relationships between the residual strength ratio R , which is the ratio of residual strength measured at strain of 0.04 to the peak stress, and two factors, the generalized diameter-to-thickness ratio α and the measured peak strain ϵ_{sm} .

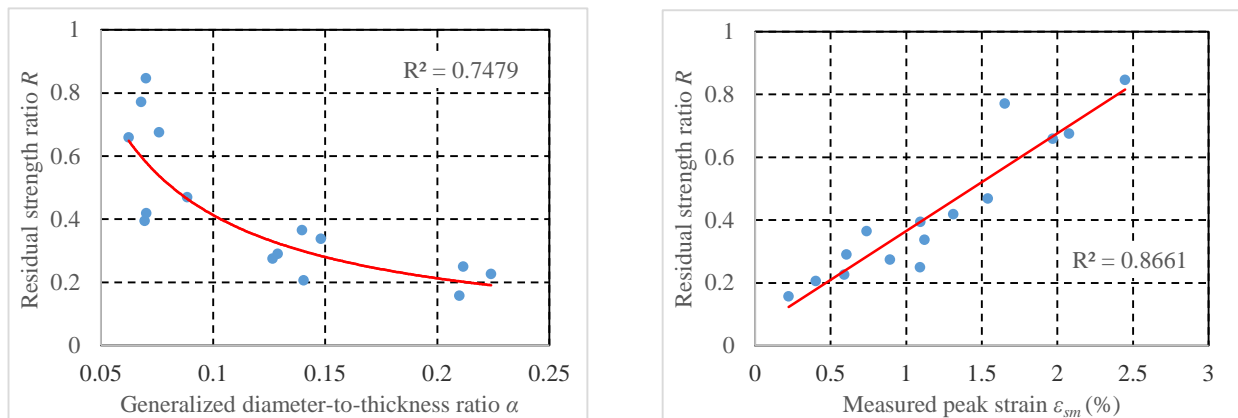


Fig. 6 – Experimental results of the residual strength ratio R



One can see from Fig. 6 that the measured peak strain ϵ_{sm} exhibits stronger correlation with the residual strength ratio R than α . Based on the results shown in Fig. 6, the following equation is derived to calculate the residual strength f_{res} at the strain of 0.04.

$$f_{res} = Rf_{sm} = (0.05 + 0.3\epsilon_{sm}) f_{sm}, \quad \epsilon_{sm} \text{ in } \% \quad (7)$$

Then the parameters governing the descending portion can be obtained as follows:

$$a = \frac{f_{res}f_{sm}(0.04 - \epsilon_{sm})}{f_{sm} - f_{res}}, \quad b = \frac{0.04f_{res} - \epsilon_{sm}f_{sm}}{f_{sm} - f_{res}} \quad (8)$$

As can be seen from Eq. (2) through Eq. (8), the proposed stress-strain model is a one-parameter model. Only if the generalized diameter-to-thickness ratio α of steel tubes is known, the local buckling strength Sf_{sy} or f_{sm} , the buckling strain ϵ_{sm} , and the stress-strain relationship for CHSS columns can be completely determined.

3. Verification of the proposed model

Fig. 7 shows comparison between the measured peak stresses and strains and the calculated results along with the statistical results. The “mean” and “St. Dev.” superimposed in Fig. 7 represent the average and standard deviation of the experimental to calculated results, respectively.

The calculated peak stresses agree very well with the experimental results. The ratio of experimental strengths to calculated ones has a mean value of 1.00, and a standard deviation of 0.07, which implies high accuracy of Eq. (4) and Eq. (6). Based on this observation, authors recommend that Eq. (4) can be used to predict the local buckling strength of CHSS columns due to its simplicity and Eq. (6) can be used to conduct intensive analysis of the seismic performance of CHSS columns.

One can also see from Fig. 7 that the experimental peak strains can be predicted by Eq. (5) with sufficient accuracy. The experimental/calculated ratios have a mean value of 1.1 and a standard deviation of 0.24. While scattering is observed between the experimental peak strains and the calculated ones, considering the instability of the peak strains due to the near-zero stiffness, these two statistical values indicate that Eq. (7) is reliable and accurate enough for practice.

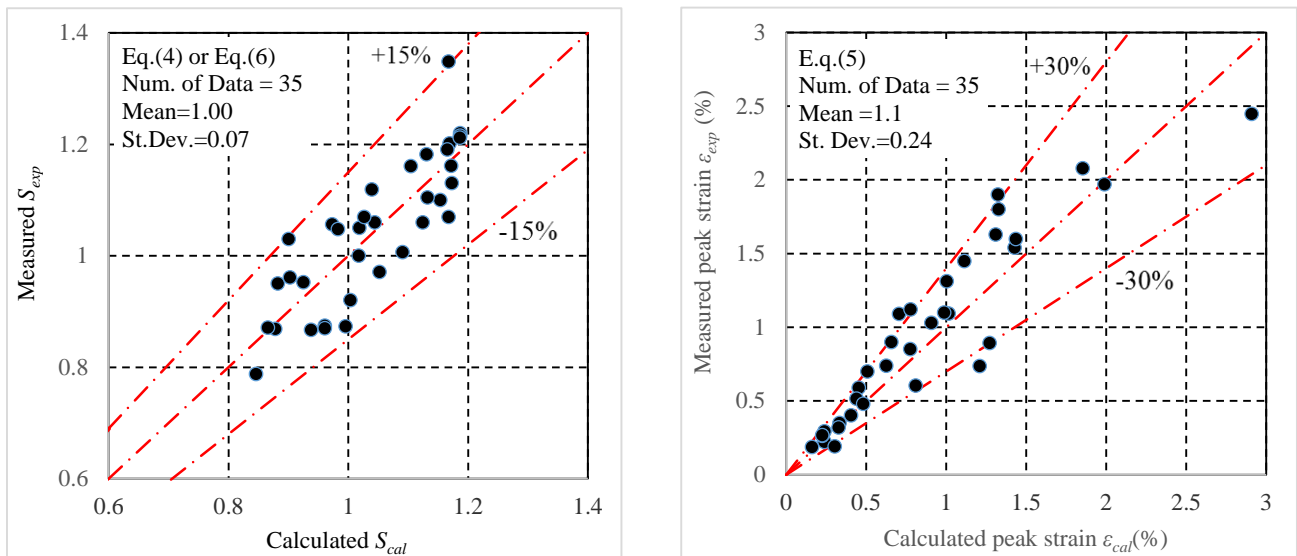


Fig. 7 – Comparisons between the measured and calculated peak stresses and peak strains



In order to examine total accuracy of the proposed model, comparisons between the measured stress-strain curves of six representative CHSS columns and the calculated ones are shown in Fig. 8. The main experimental parameters of these columns are listed in Table 1.

Table 1 – Main variables of representative specimens

Notation	D (mm)	f_y (Mpa)	D/t	L/D	α	Ref. No.
NO.1	122	579	26.9	3	0.076	[12]
NO.2	149	283	50.3	3	0.069	
NO.3	360	579	79.3	3	0.224	
NO.4	318.5	514.5	77.7	3	0.195	[13]
NO.5	301	283	101.7	3	0.140	[12]
NO.6	450	283	152.0	3	0.210	

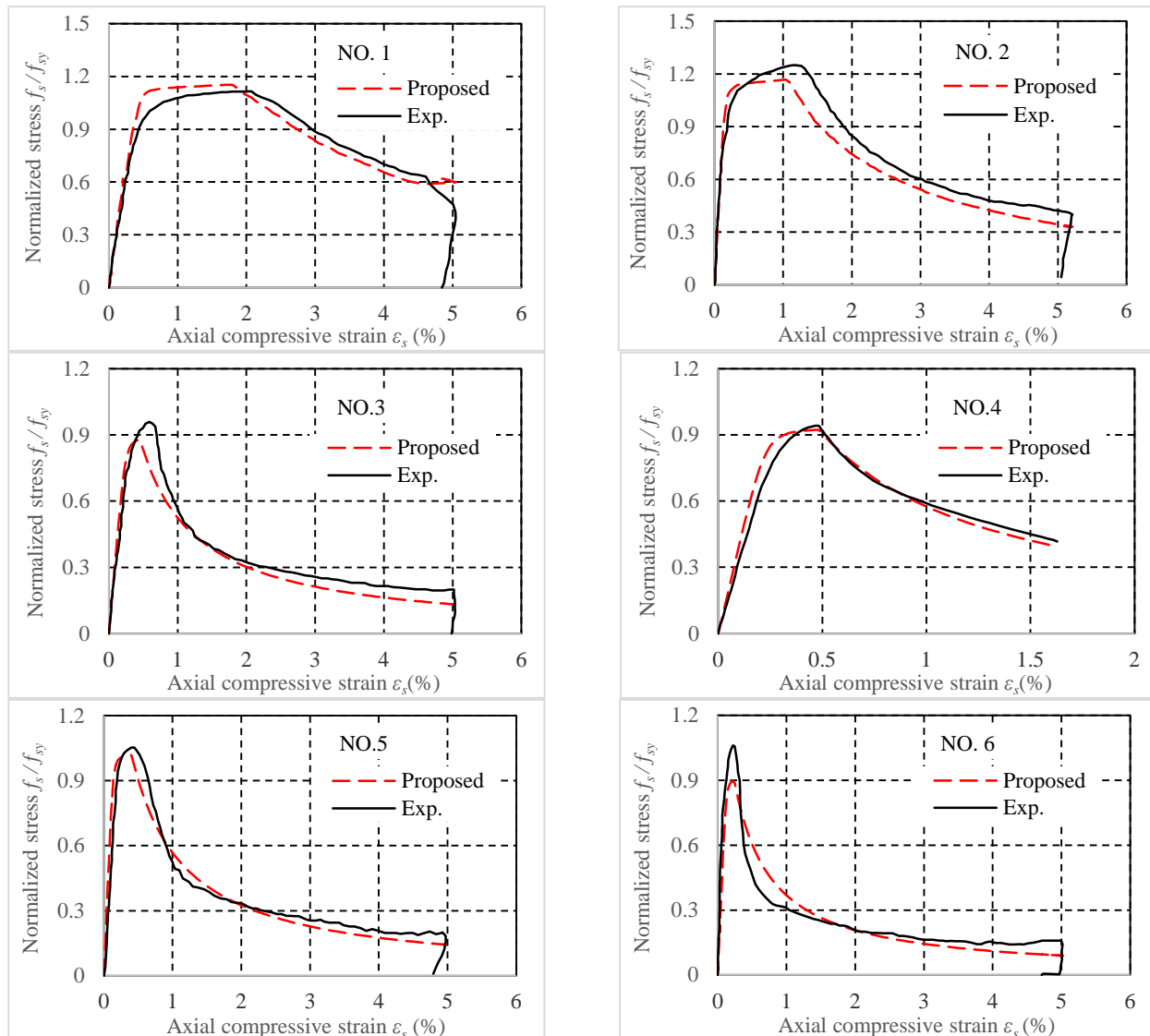


Fig. 8 – Comparisons of experimental and calculated stress-strain curves of CHSS columns



One can see from Fig. 8 that the calculated stress-strain curves by the proposed model agree well with the measured results up to larger strain. The proposed model can trace not only the nonlinearity caused by residual stress on the ascending portion of the stress-strain curve, but also the post-local-buckling behavior with very high accuracy.

To further verify the accuracy of the proposed model, Fig. 9 compares the areas covered by the measured stress-strain curves prior to the last unloading strain with those covered by the calculated stress-strain curves in terms of the relationship between the experimental-to-calculated area ratios. The experimental-to-calculated area ratio has a mean of 0.95, and a standard deviation of 0.15, which implies sufficient high accuracy for practice.

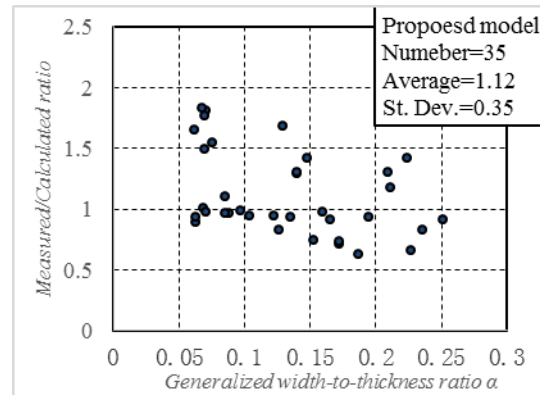


Fig. 9 – Overall accuracy of the proposed model

5. Conclusions

In this paper, a stress-strain model is proposed to predict the compressive stress-strain behavior of cold-formed circular hollow steel stub columns. The proposed model can account not only for the effect of nonlinearity due to residual stress induced during manufacturing process, but also for the effect of elastic and inelastic post-local buckling on the stress-strain performance of CHSS columns under compression.

In order to verify validity and accuracy of the proposed model, the test results of thirty-five CHSS columns conducted by many researchers have been collected and used. Through comparisons between the experimental results and the calculated ones, the following conclusions can be drawn:

(1) The proposed model can predict stress-strain behavior of circular hollow steel stub columns under compression up to large strain very well.

(2) The local buckling strength and buckling strain where elastic or inelastic local buckling commences can be predicted with very high accuracy by Eq. (4) and Eq. (5), respectively.

(3) The proposed model is a one-parameter model. Only if the generalized diameter-to-thickness ratio (α) is known, the compressive stress-strain relation of CHSS columns can be completely determined.

(4) Due to its simplicity and accuracy, the proposed model enables structural engineers to conduct reliable prediction of seismic performance of steel structures made of CHSS columns under stronger earthquake than anticipated in current seismic design codes. In addition, the proposed model can open a way for researchers to study the axial behavior of circular concrete-filled steel tubular columns with higher reliability.

References

- [1] Central Disaster Prevention Council of Japan (2011): Interim report on the Nankai-trough mega-earthquake. http://www.bousai.go.jp/jishin/nankai/model/pdf/chukan_point.pdf.



- [2] AISC(1996): Load and resistance factor design specification for structural steel buildings. American Institute of Steel Construction, Chicago.
- [3] AS 4100(1998): Steel structures. *Standards Association of Australia*, Sydney.
- [4] Eurocode 3 Part 1.3 (1992): Design of steel structures: part 1.3-Cold-formed thin gauge members and sheeting, CEN/TC250/SC3-PT1A, 3rd edition.
- [5] AIJ (1990): Recommendations for the design and fabrication of tubular structures in steel. *Architectural Institute of Japan*, Tokyo.
- [6] GB50017 (2003): Code for design of steel structures. *China architecture & building press*. Beijing. [in Chinese]
- [7] Yamada S, Akiyama H, Kuwamura H (1993): Post buckling and deteriorate behaviour of box-section steel members. *Journal of Structure and Construction Engineering*. **444**, 135-143. [in Japanese]
- [8] Yamada T, Ishida T, and Shimada Y (2012): Hysteresis model of RHS Columns in the deterioration range governed by local buckling. *Journal of Structure and Construction Engineering*. **674**,627-636. [in Japanese]
- [9] Sakino K, Nakahara H, Morino S, and Nishiyama I. (2004): Behavior of centrally loaded concrete-filled steel-tube short columns. *Journal of Structural Engineering*. **130**(2), 180-188.
- [10] Kato B, Akiyama H, Suzuki H. (1973): Plastic local buckling capacity of steel tubes under axial compression. *Journal of Structure and Construction Engineering*. **204**, 9-17.
- [11] Kato B. (1995): Compressive strength and deformation capacity of concrete-filled tubular stub-columns – Part 1 Strength and rotation capacity of concrete-filled tubular columns. *Journal of Structure and Construction Engineering*. **468**,183-191 [in Japanese].
- [12] T. Fujimoto, A. Mukai, I. Nishiyama, ect. (1997): Axial comprehensive behavior of concrete filled steel tubular stub columns using high strength material. *Journal of Structure & Construction Engineering*. 498,161-168. [in Japanese]
- [13] Kato B. (1987): Deformation capacity of tubular steel members governed by local buckling. *Journal of Structure and Construction Engineering*. **378**, 27-36. [in Japanese]
- [14] Martin D., O'shea, Q. Bridge (1997): Local buckling of thin-walled circular steel sections with or without internal restraint. *Journal of constr58ctional steel research*. **41**,137-157.
- [15] T. Suzuki, S. Motoyui, H. Ohta. (1996): Buckling and post buckling behavior of concrete filled rectangular steel tubular stub columns under pure axial comprehension. *Journal of Structure & Construction Engineering*. **486**,143-151.
- [16] Menegotto, M, and Pinto, RE. (1973): Method of analysis for cyclically loaded RC plane frames including changes in geometry and non-elastic behavior of elements under combined normal force and bending. *Proc. of LABSE Symposium on Resistance and Ultimate Deformability of Structures Acted on by Well Defined repeated loads*. **13**, 15-22.
- [17] Sun Y, Fukuhara T, and Kitajima H. (2006): Analytical study of cyclic response of concrete members made of high-strength materials. *Proceedings of the 8th National Conference on Earthquake Engineering*, San Francisco, California.
- [18] Hayashi M, Tauchi T, Fukumoto T, and Saeki T. (1993): Axial behavior of concrete-filled square tubular columns made of high-strength materials. *Proceedings of Japan concrete institute*. **15**(2), 977-982. [in Japanese]